Processing and Characterizations of Eucalyptus-PA12 Composite by Laser Sintering

Kaiyi Jiang[1,2] ,Yanling Guo[1*], David L. Bourell[2*]
[1.] College of Mechatronics Engineering, Northeast Forestry University, Harbin 150040, P.R.CHINA
[2.] Laboratory for Freeform Fabrication, The University of Texas at Austin, TX 78712-0292, USA

Abstract

To meet the existing requirements to make Laser Sintering (LS) technology more economical and environmentally friendly, a new type of low cost sustainable material (eucalyptus-polyamide 12 (EPA12) composite) was developed. This paper presents initial research into the LS PA12 with wood powder additions.

EPA12 mixed in a ratio of 1:2 by volume has been shown to be extremely processable by LS. Before sintering experiments, thermal conductivity (which is an important component in understanding and optimizing the processing of laser sintering EPA 12) was measured. During LS processing, a variety of laser powers were chosen to investigate the effect of the energy input on the densification, mechanical properties and forming accuracy of the material. The dispersion of eucalyptus in the LS specimens of the composite powder was examined by scanning electron microscopy (SEM). The microstructure of sintered EPA12 was observed. By comparing the microstructures, observable differences based on varying levels of laser power were also present. The maximum tensile strength and the flexure strength of prototypes are 3.7 MPa and 38 MPa, respectively. These values increased from the minimum with increased energy input. On the contrary, the forming accuracy was high at a relatively low laser power.

Introduction

Additive Manufacturing (AM) or 3D printing is a process of making a three-dimensional solid object of virtually any shape from a digital model. Instead of standard 'subtractive manufacturing'-where material is cut away from a single piece-AM involves building up a part from a series of layers, each one printed on top of the other.

In AM, stereolithography (SLA) [1], selective laser sintering or laser sintering (SLS or LS) [2], fused deposition modeling (FDM) [3] and three-dimensional printing (3DP) [4], etc. are the main commercial systems available on the market. But these systems all have a limit on the type and properties of materials that can be fabricated. SLS originally developed at the University of Texas at Austin has attracted much attention because of its wide range of material selection. The available feedstock of LS includes polycarbonate (PC), nylon, nylon/glass composite, wax, ceramics, elastomeric and metal-polymer powder.

Very limited effort has been made to develop sustainability in AM such as sustainable principles, materials, application and practices to enable environmentally benign, economically

advantageous and societal benefit-driven AM methodologies as well as to make this technology more affordable [5]. The goal of this research was to develop a type of low-cost sustainable and natural material for LS.

In this paper, the composite being considered is composed of eucalyptus and PA12. PA12 is a mature commercially available material with good laser processing properties. Therefore, It was selected as the matrix and binder for eucalyptus which is a variety of wood powder. The initial experiments and analyses showed the feasibility of laser sintering EPA12 composite.

Experiment and Procedures

1 Materials

The material used in this research consisted of composite material made from polyamide with wood flour additive. The wood flour is 300 micron mesh eucalyptus powder from De Long New Materials Co., Ltd in JIANGXING China. Polyamides 12 (PA 12), also called Nylon 12 was obtained from Advanced Laser Materials, LLC. Some of the material specifications are listed in Table 1.

Table 1 Material Specifications

Properties	Eucalyptus	PA12
Particle Size Range	10-100µm	40-80µm
Particle Shape	Irregular	Irregular
Embodied Energy	4.22e3-4.69e3 BTU/lb	6.19e4-6.84e4 BTU/lb
Specific Heat Capacity	0.396-0.408 BTU/lb. ºF	0.401-0.411 BTU/lb. ºF
Thermal Conductivity	0.0792-0.0965 BTU.ft/hr.ft^2. ºF	0.126-0.177 BTU.ft/hr.ft^2. ºF
Melting Temperature	N/A	338-352 ºF

In this research, both materials were sifted through a 70 mesh intensive shaking procedure, using a VORTI-SIV sifter to remove powder agglomerates. Figure 1 shows particle size distributions obtained after sieving by laser diffractometry. Following the sifting, the wood powder and PA12 were mechanically mixed to a volume ratio of 1:2 in a ceramic grinding jar using a U.S. Stoneware 803 DVM Long Roll Jar Mill. To obtain homogeneous powder mixtures of uniform color and maximum dispersion, the powder was mixed at high speed for 5 hours with small cylindrical ceramic grinding media. Ceramic media offer high purity grinding and reduced grind time. The homogeneous mixed powder was removed from the jars.

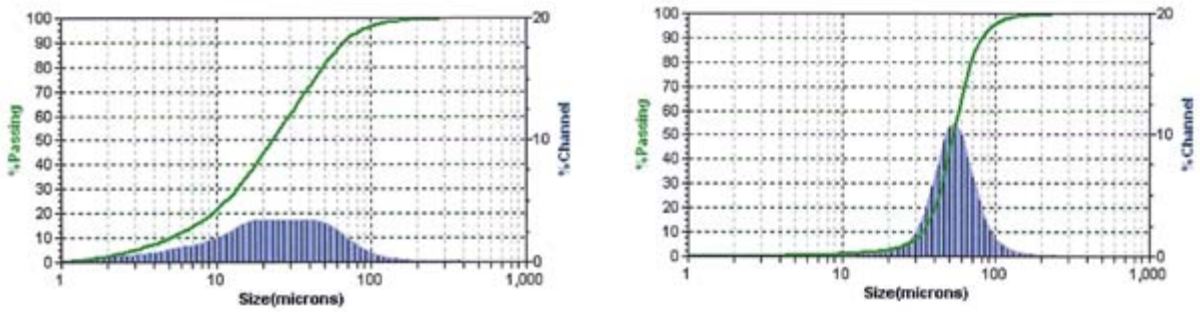

(a) eucalyptus (b) PA12

Fig.1 Particle size distributions

2 Thermal conductivity measurement

Apparatus: A plane-source transient thermal conductivity measurement machine (HotDisk® TPS 500) and a temperature control oven were acquired, which are shown in Figure 2. A powder holder was fabricated, allowing the conductivity probe to be sandwiched between two sections of powder. The interstitial gas was heated through the copper tubes that were hung on the inside wall [6].

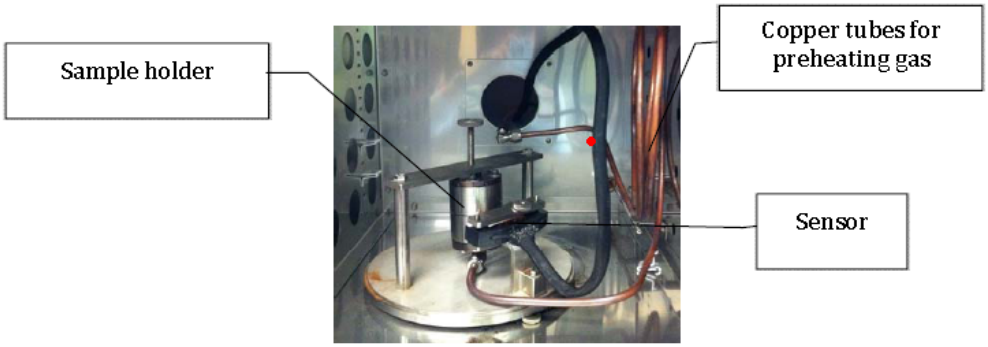

Fig. 2 Experimental apparatus for measuring the thermal conductivity

The mixed EPA12 powder was loaded into the sample holder and tapped to settle it before the measurement. Because the melting point of PA12 is 180 ℃, and the previous processing was generally at a part bed temperature of 174 ℃, the testing started at 30℃ and ended at 174℃. A 10 ℃ increment was selected.

At each temperature, eight individual measurements were made, each of which lasted 80 seconds. Fifteen minutes separated each measurement, allowing the sample to reach a steady state. It took 2~3 hours to reach an equilibrium state at each temperature. The heating power was 60 mW with an electrical frequency of 60 Hz. The sensor material was Kapton, with a radius of 6.403 mm. The available probing depth was 12.00 mm.

The 80-second experiment time included a 40 s drift time and 40 s testing time. The measured sensor temperature before heating showed small variations, which indicated the equilibrium state. The transient graph shows the temperature increases 1-3K. The first 50 points are ignored in that

the temperature increases too quickly in a short time, while 51-200 points are selected, which perform a smoothly increasing straight line.

3 Laser Sintering

Specimens of EPA12 mixtures in the volume ratio of 1:2 were produced by using a DTM Sinterstation® HiQ. Processing parameters were 10 W, 15 W, 20 W, 25 W, 30 W CO2 laser, with a scan speed of 2000 mm/s, scanning space of 0.15 mm, layer thickness of 0.1~0.2 mm and the powder bed temperature of 174 ℃.

4 Mechanical analysis

An instron mechanical testing machine was used for mechanical property testing.

Dog-bone-shaped tensile specimens having a typical dimension of 165 ×13 × 4 mm, were tested according to ASTM D638. A crosshead speed of 5 mm/min and a gage length of 80 mm were used for the test.

5 Scanning electron microscopy (SEM)

The microstructures of the surface of the EPA 12 specimens in the Y-direction and the cross-section of the fractured parts in the Z-direction were observed using SEM to investigate the binding mechanism, the fracture surface, the particle features and the microstructure. The specimens were sputtered with gold by SEM specimen coating equipment, as the materials are non-conductive.

Results and Discussion

1 Powder Morphology

Figure 3 shows SEM micrographs for neat PA 12, the eucalyptus fibers and low and high magnification images of EPA12 blend mixed at a ratio of 1:2 (by volume). As shown in Figure 3a, the shape of the neat PA 12 powder is irregular with a uniform size and a rough surface. From Figure 3b, eucalyptus fibers present a rough surface with an irregular shape such as flaky, acicular and flocculent, and the fiber sizes are not uniform. Figures 3c and 3d show that the distribution of the eucalyptus fiber and PA12 powder is uniform. Eucalyptus fibers are randomly cluttered among PA12 particles. Moreover, the high aspect ratio of the fiber can enlarge the contact area of wood fibers and PA12 particles, which can also enhance the bonding capacity of the interface between the fiber and PA12 during sintering.

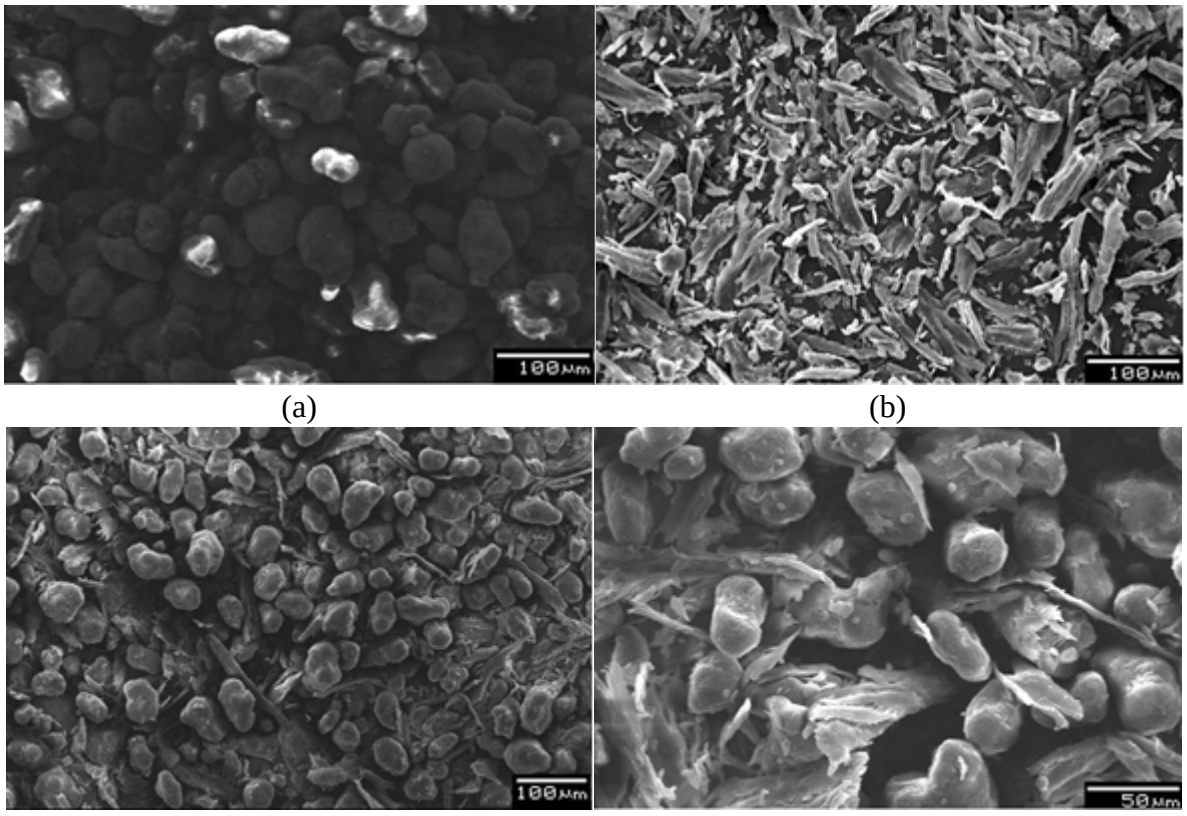

(a) (b)

(c) (d)

Fig. 3 SEM Micrographs of (a) Neat PA 12 magnified by 200 times (b) Neat eucalyptus powder magnified by 200 times (c) blend magnified by 150 times (d) blend magnified by 400 times

2 Thermal Conductivity

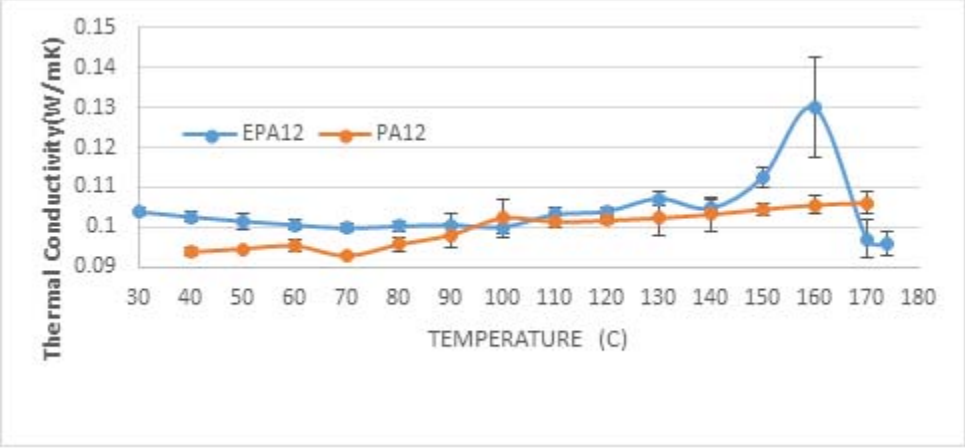

Fig. 4 Thermal conductivity of PA12 and EPA12

The comparison of the thermal conductivity of the PA12 and EPA12 powders are shown in Figure 4. It can be seen that as the temperature rise, the thermal conductivity of neat PA12

increased slightly, while, because wood fiber generally contains two parts of water, one is adsorbed from air and the other is held as molecules of water on the cellulose/lignin structure, even after air drying, wood still contains 12-18% of adsorbed water [7]. So as the temperature rose to 100 ℃, the absorbed water was evaporated, resulting in a more or less decline in thermal conductivity. With the temperature steadily increasing, the thermal conductivity of EPA12 ascended and reached a peak of 0.13 W/mK at 160 ℃. When the temperature went to higher than 160 ℃, part of the wood fibers were carbonized [7], which decreased the thermal conductivity of EPA12 dramatically. At 170 ℃ and174 ℃ (which is the processing temperature) low thermal conductivity can lead to a more accurate EPA12 laser sintering, because the laser and sintered part would have a weak impact on the surrounding un-sintered powder.

3 Laser Sintering Processing

Fig.5 Demonstration part processed using DTM Sinterstation HiQ® (Laser Power: 24 W, Scanning Speed: 2000 mm/s, Scanning Space: 0.15 mm, Layer Thickness: 0.127 mm, Part Bed Temperature: 174 ℃) in Ratio of 1:2 eucalyptus/PA12

During processing, the EPA12 composite showed good flowability and formability. A demonstration part is shown in Figure 5. The features are dimensionally articulated and reasonably sharp.

4 Forming Accuracy

Comparing designed dimensions in the model and actual dimensions of sintered parts in X, Y, Z directions, respectively, the dimensional accuracies were investigated and shown in Figure 6. It can be seen that laser power has little effect on the dimensional accuracy in X direction, which remains above 98%. In Y and Z direction, as the laser power increased from 10W to 20W, the dimensional accuracy rose slightly; however, when laser power is higher than 20W, the accuracy in both Y and Z direction dramatically decreases to under 92% when the laser power is 30W, which is lower than 92.1%-the dimensional accuracy of laser sintered neat PA12 [8]. It indicates

that under a high energy input associated with the part bed temperature and laser power, EPA12 will have more shrinkage than neat PA12.

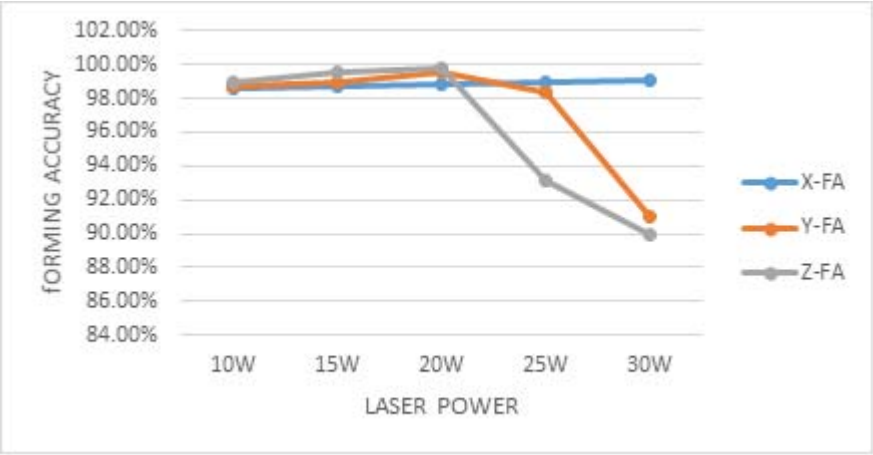

Fig. 6 Forming accuracy of laser sintered EPA12

5 Mechanical Properties

Figures 7 (a), (b) show the tensile strength and Young's modulus results obtained in relation to various laser powers. It is clear that the tensile strength and Young's Modulus increased rapidly with an increase in laser power, but when the laser power exceeds 25 W, the tensile strength keeps almost steady and there is a slight raise in Young's Modulus. Judging from the results obtained, the strength is directly influenced by part-density, which is in turn affected by energy input associated with laser power and part bed temperature (Part bed temperature is constant at 174 ℃ in this paper). Density and tensile strength are in direct proportion to each other. Therefore, high laser power causes more extensive wetting by the PA12 on eucalyptus fibers, which further improves the part-density and bonding strength as well as the tensile strength and the Young's modulus. This is the result of enhanced fusion of Polyamide 12 particles and a decrease in porosity to produce a more compact structure. With degradation of the Polyamide 12 particles due to excessively high ED, the tensile strength declines directly. Compared with the tensile strength of eucalyptus/PES and Rice-husk/PES parts after post-processing which are 1.21 MPa [9] and 1.47 MPa [10], respectively, the strength of green EPA12 part is higher than others, suggesting that as the matrix, PA12 has a better wettability on eucalyptus fibers than PES. However, compared with neat PA12, the strength of EPA12 is much lower, which indicated weak polymer-filler interaction.

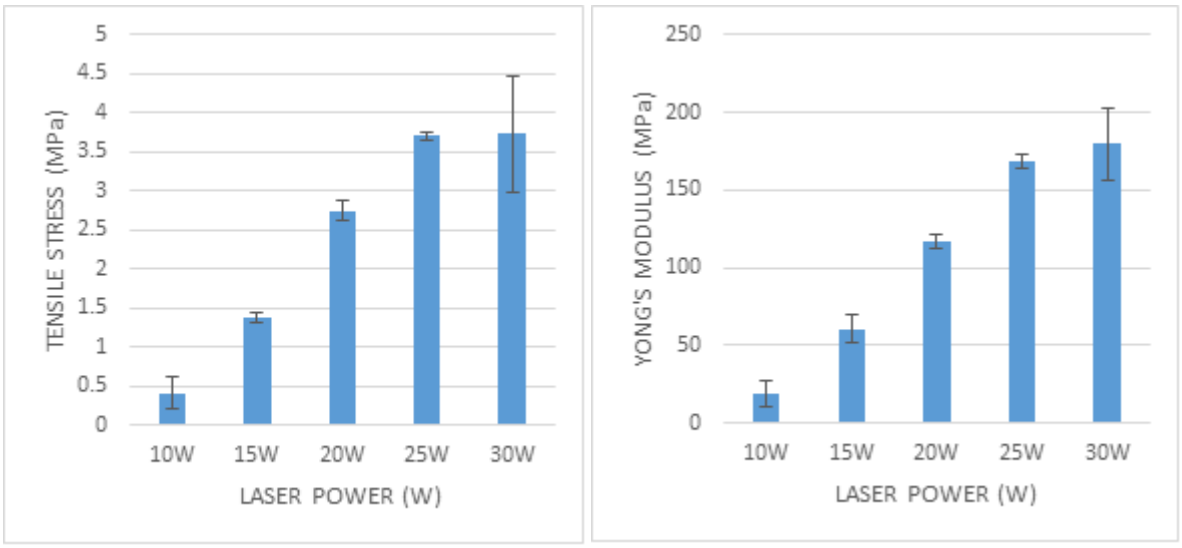

(a) (b)

Fig. 7 Effect of laser power on (a) tensile stress and (b) Young's Modulus

6 Microstructure Observation

Using scanning electron microscopy, the microstructures of the surfaces and cross-sections of EPA12 parts sintered by different laser powers were observed as shown in Figures 8 and 9. It can be seen that for both surfaces and cross-sections, eucalyptus fiber was dispread evenly in the PA12 matrix, and no agglomeration occurred.

However, at a low laser power (10W), both the surface and the cross-section microstructures show that the powders were in a relative loose state. There are large holes, many unsintered PA12 particles and partly wetted wood fibers observed in the part (as shown in Figure 8(a) and Figure 9(a)). Some un-coated fibers adhered to the surface the small continuous phrase of PA12. This indicates that low laser power does not provide enough energy for PA12 to melt and bond the surrounding fiber. This results in a weak internal bonding force and an external low strength.

By increasing the laser power, there are less and less holes and loose powder in the part. More PA12 particles were melted, and this resulted in more wood fiber being tightly joined by an extensive continuous phase formation. This indicated the sufficient melt flow of PA12 under a high laser power processing and a good interfacial adhesion between wood fiber and PA12.

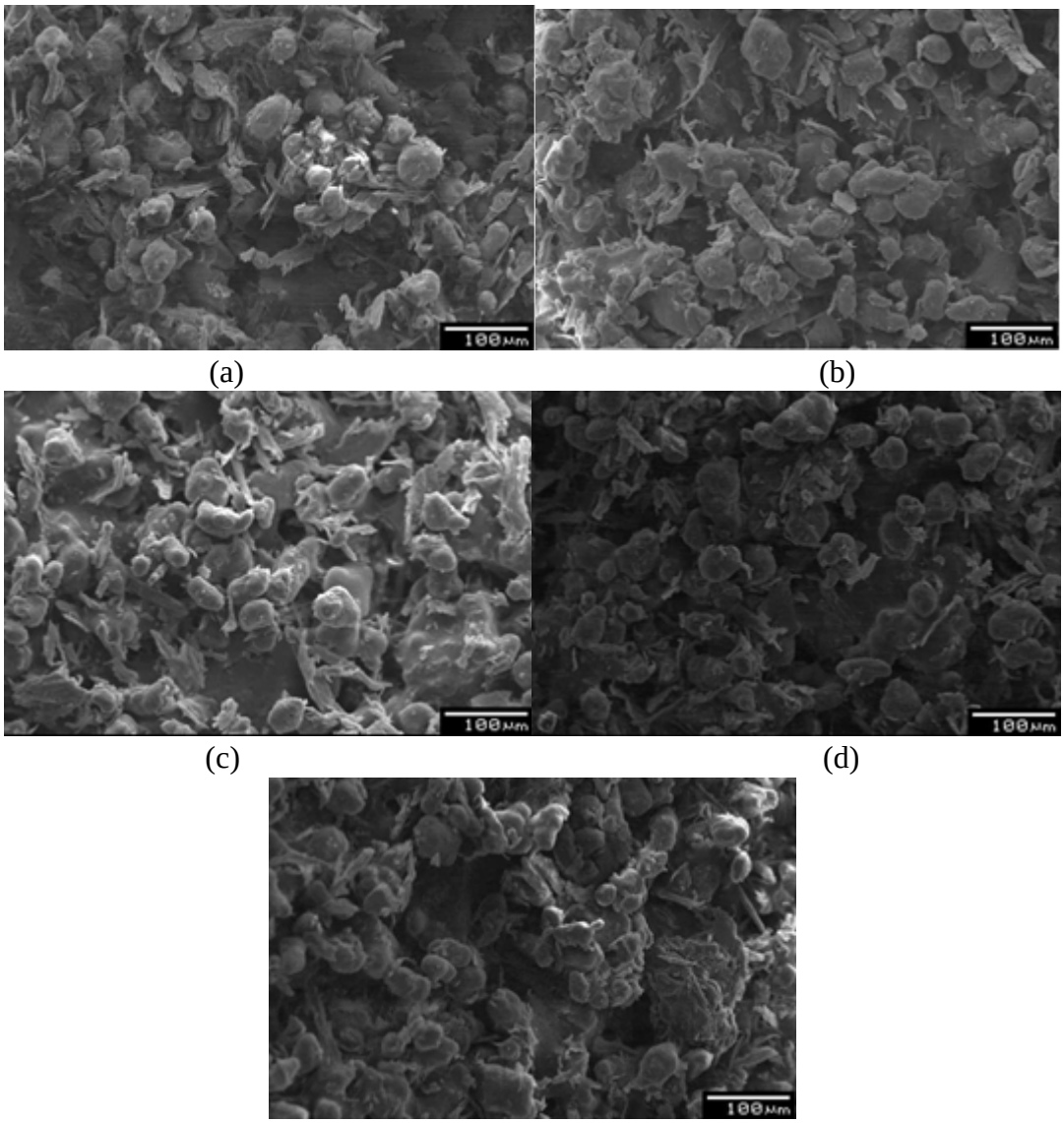

(a) (b)

(c) (d)

(e)

Fig. 8 SEM photos of EPA 12 part surfaces magnified by 200 times (a) built by 10 W of laser power; (b) built by 15 W of laser power; (c) built by 20 W of laser power; (d) built by 25 W of laser power; (e) built by 30 W of laser power

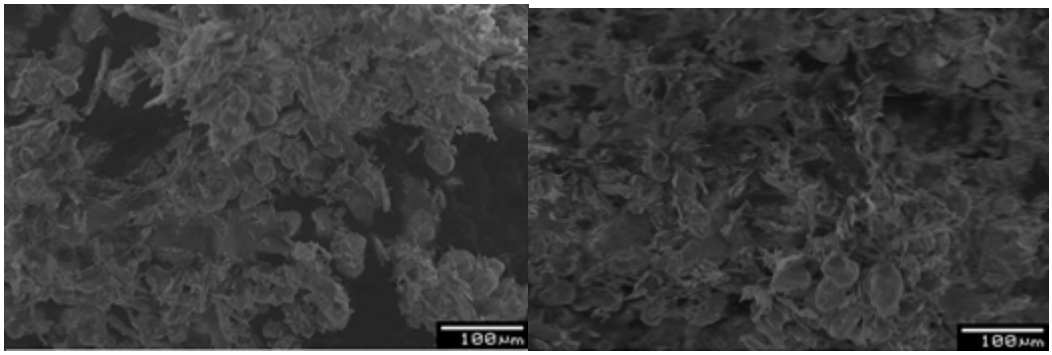

(a) (b)

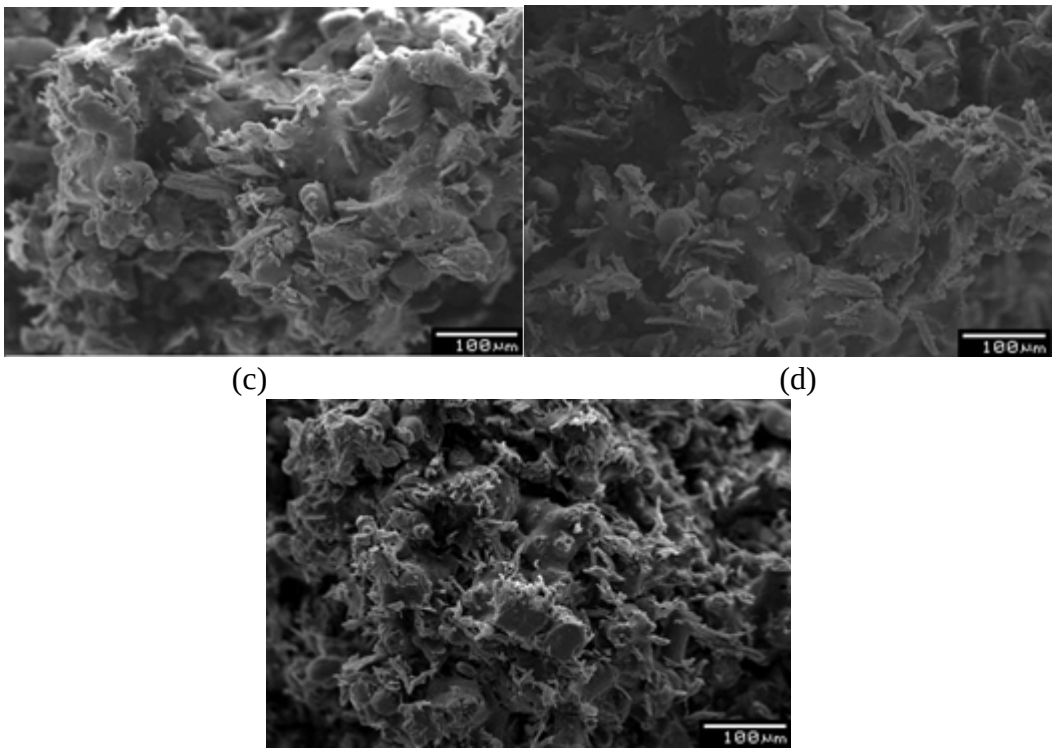

(c) (d)

(e)

Fig. 8 SEM photos of EPA 12 part cross-sections magnified by 200 times (a) built by 10 W of laser power; (b) built by 15 W of laser power; (c) built by 20 W of laser power; (d) built by 25 W of laser power; (e) built by 30 W of laser power

Conclusions

A new type of sustainable material, a mixture of eucalyptus and polyamide 12 powder, was developed and used in LS in this research. The material shows promise as a feedstock that is green, natural and environmentally friendly with high mechanical strength, good flowability and formability. The suitable mixing ratio of EPA 12 was 1:2 by volume, which can ensure most eucalyptus fibers can be wet and bonded together by PA12. Laser sintered EPA12 parts showed more dimensional accuracy than PA12 parts due to the low thermal conductivity of EPA12 at the processing temperature of 170℃ to 174℃. Tension testing results showed the strength of EPA12 parts increased with an increase laser power. It is higher than the strength of eucalyptus/PES parts and rice-husk/PES, but lower than neat PA12 parts.

In conclusion, the manufacturing of a eucalyptus/PA12 blend using a laser sintering process demonstrates that it is possible to use a low-cost and sustainable composite in additive manufacturing to produce parts with good mechanical properties.

Acknowledgments

This work was supported by National Natural Science Foundation of China (51075067), China Scholarship Council.

References

[1] Melchels, FPW, Feijen J, Grijpma DW.. 2010, “A review on stereolithography and its applications in biomedical engineering”, Biomaterials. Vol31, pp. 6121-6130.
[2] Haseung Chung, Suman Das. 2006, “Processing and properties of glass bead particulate-filled functionally graded Nylon-11 composites produced by selective laser sintering”, Materials Science and Engineering: A, Vol. 437, pp. 226-234.
[3] Calvert P., Crockett R., Lombardi J., et al. 1994, “Extrusion method for solid freeform fabrication”, In Proceeding of the Solid Freeform Fabrication Symposium, pp. 50-55
[4] Seitz H., Rieder W., Irsen S., et al. 2005, “Three-dimensional printing of porous ceramic scaffolds for bone tissue engineering”, JOURNAL OF BIOMEDICAL MATERIALS RESEARCH PART B-APPLIED BIOMATERIALS, Vol. 74B, pp. 782-788.
[5] David L. Bourell, Ming C.Leu and David W. Rosen, 2009, “Roadmap for Additive Manufacturing”, The University of Texas at Austin, Laboratory for Freeform Fabrication, Advanced Manufacturing Center, Austin, TX.
[6] Mengqi Yuan, David Bourell, Tim Diller. 2011, “Thermal Conductivity Measurement of Polyamide 12”, In Proceeding of the Solid Freeform Fabrication Symposium, pp.427-437
[7] Introduction to the Wood carbonization, Baidu Library. http:// wenku.baidu.com/ in Chinese.
[8] Jiaming Bai, Ruth D Goodridge, Richard JM Haque. “Carbon nanotube reinforced Polyamide 12 nanocomposites for laser sintering”, In Proceeding of the Solid Freeform Fabrication Symposium, pp.98-107
[9] Kaiyi Jiang, Study on the Experiment and the Post Processing of the Wood Plastic Composite Based on Selective Laser Sintering, Master thesis, Northeast Forestry University, Harbin, Heilongjiang, China, 2011.
[10] Weiliang Zeng, Yanling Guo, Kaiyi Jiang, et al., Preparation and Selective Laser Sintering of Rice Husk-Plastic Composite Powder and Post Processing, Digest Journal of Nanomaterials and Biostructures, 7(3) (2012), 1063-1070.